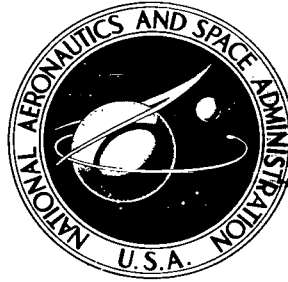


NASA TECHNICAL NOTE



NASA TN D-4970

C.1

NASA TN D-4970

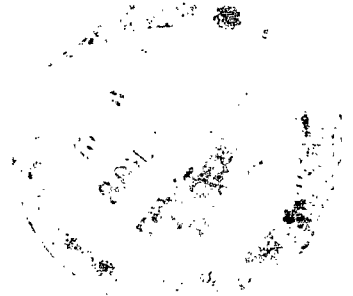


LOAN COPY: RETURN TO
AFWL (WLIL-2)
KIRTLAND AFB, N MEX

ELECTRICAL RESISTIVITY AS A FUNCTION OF DEUTERIUM CONCENTRATION IN PALLADIUM

*by Gust Bambakidis, Robert J. Smith,
and Dumas A. Otterson*

*Lewis Research Center
Cleveland, Ohio*





ELECTRICAL RESISTIVITY AS A FUNCTION OF DEUTERIUM
CONCENTRATION IN PALLADIUM

By Gust Bambakidis, Robert J. Smith, and Dumas A. Otterson

Lewis Research Center
Cleveland, Ohio

NATIONAL AERONAUTICS AND SPACE ADMINISTRATION

For sale by the Clearinghouse for Federal Scientific and Technical Information
Springfield, Virginia 22151 - CFSTI price \$3.00

ABSTRACT

The electrical resistivity of the palladium-deuterium system was measured to a deuterium- to palladium-atom ratio of 0.9 at temperatures of 273, 77, and 4.2 K. The resistivity ratio $\rho(x)/\rho(0)$ was plotted as a function of the atom ratio x at 273 and 4.2 K. A modification of Mott's model for the resistivity of transition-metal alloys was used to calculate the structural resistivity. A good fit to the data at 4.2 K was obtained by assuming that the number of d-holes per palladium atom takes on the value of 0.55 to 0.60 on addition of deuterium.

ELECTRICAL RESISTIVITY AS A FUNCTION OF DEUTERIUM CONCENTRATION IN PALLADIUM

by Gust Bambakidis, Robert J. Smith, and Dumas A. Otterson
Lewis Research Center

SUMMARY

The electrical resistivity of the palladium-deuterium (Pd-D) system was measured to a deuterium- to palladium-atom ratio of 0.9 at temperatures of 273, 77, and 4.2 K. The resistivity ratio $\rho(x)/\rho(0)$ was plotted as a function of the atom ratio x at 273 and 4.2 K. A modification of Mott's model for the resistivity of transition-metal alloys was used to calculate the structural resistivity. A good fit to the data at 4.2 K was obtained by assuming that the number of d-holes per Pd atom takes on the value of 0.55 to 0.60 on addition of D.

INTRODUCTION

At room temperature, deuterium (or hydrogen (H)) occupies the octahedral interstitial sites of the face-centered-cubic Pd lattice (refs. 1 and 2). The octahedral sites are occupied for both α -Pd and β -Pd, with the D/Pd and H/Pd atom ratios ranging from 0 to 0.72 (where α -Pd and β -Pd have lattice constants of 3.86×10^{-8} and 4.02×10^{-8} cm, respectively). Denoting the D/Pd or H/Pd atom ratios by x reveals that only α -Pd exists for $0 < x \lesssim 0.02$. For $0.02 \lesssim x \lesssim 0.60$, α -Pd and β -Pd coexist, and only β -Pd exists for $x \gtrsim 0.60$. If $\rho(x)$ is the resistivity of PdH_x (or PdD_x) and $\rho(0)$ the resistivity of annealed Pd, the resistivity ratio $[\rho(x)/\rho(0)]_{298\text{K}}$ and its derivative increase for increasing x at $0.02 \lesssim x \lesssim 0.70$. The resistivity ratio is a maximum for $x \approx 0.76$, and the ratio along with its derivative decreases for $0.76 \lesssim x \leq 0.88$ (ref. 3). In the PdD_x system, the available data show that the ratio $[\rho(x)/\rho(0)]_{298\text{K}}$ and its derivative increase from $x \approx 0.02$ to $x = 0.67$ with no higher values of x being shown (ref. 4). For pure α -Pd ($x \lesssim 0.02$), the derivative of the resistivity ratio $[\rho(x)/\rho(0)]_{298\text{K}}$ is larger than that for the α -Pd + β -Pd phase for either PdH_x or PdD_x .

The objective of the present work is to extend the resistivity data for PdD_x beyond $x = 0.67$ to see if, in the plot of $\rho(x)/\rho(0)$ as a function of x , a maximum occurs similar to that found for PdH_x at 273 K. The thermal contribution to the resistivity was minimized by obtaining data at 4.2 K, and then a modification of Mott's model for the resistivity of transition-metal alloys (ref. 5, p. 296) was used for the analysis of the structural contribution. The resistivity results and analysis presented herein for the PdD_x system should be qualitatively applicable to the PdH_x system since these systems are quite similar in other resistive and crystallographic properties thus far investigated (refs. 1 to 4 and 6 to 8).

EXPERIMENTAL PROCEDURE

The experimental data were obtained at 4.2, 77, and 273 K. Obtaining the 4.2 K data necessitated rapidly cooling or quenching the PdD_x wires from 273 to 4.2 K to prevent the migration of deuterium ions from their octahedral sites (0, 0, 1/2; 0, 1/2, 0; 1/2, 0, 0; . . .) to their tetrahedral sites (1/4, 1/4, 1/4; 3/4, 3/4, 3/4; . . .). For PdH_x , an analysis of the data for neutron diffraction and that for resistivity as a function of temperature $\rho(T)$ showed that up to 25 percent of the hydrogen may migrate to tetrahedral sites. These octahedral-tetrahedral transitions occur for PdH_x at $0.45 < x < 0.75$ if the PdH_x wires are cooled without quenching (refs. 6 and 7). In the PdH_x system, the octahedral-tetrahedral transitions may begin well above 100 K and continue at least to the neighborhood of 50 K (at which point a maximum in the resistivity and specific heat occurs) as the temperature is lowered from 273 to 4.2 K (ref. 6). (Whether or not additional transitions occur below these maximums is not known.) Although no neutron diffraction data are available for PdD_x , the resistivity data of PdD_x are almost identical to those obtained for PdH_x between 273 and 4.2 K (ref. 8). However, at a given temperature, the octahedral-tetrahedral transitions take much longer in the PdD_x system (up to several hours) than in the PdH_x system (not more than a few seconds). From these data for PdD_x , one can conclude that rapid cooling of the PdD_x specimens from 298 to 4.2 K, as employed in the present experiments, was sufficient to prevent a significant amount of deuterium migration to the tetrahedral sites.

Wire specimens of 99.995 atomic percent Pd (manufacturer's stated purity) and 0.254-millimeter diameter were annealed by joule heating in a vacuum of 5×10^{-9} torr at approximately 1200 K for at least 0.5 hour. Measurements of initial resistivity $\rho(0)$ were made at 4.2, 77, 273 K by using the conventional four-probe potentiometric technique in which a phenol formaldehyde specimen holder utilized phosphorbronze spring contacts for the current and potential contacts to the specimen. Six potential contacts, spaced 1 centimeter apart between the current contacts, permitted five consecutive

measurements along the wire. This spacing allowed the detection of resistance irregularities due to preabsorption conditions and/or nonuniform absorption along the wire after deuterium absorption. The measuring currents used were 10 milliamperes in all cases

Deuterium absorption was accomplished electrolytically with a graphite anode and a Pd-wire cathode in a 1-normal solution of deuterium sulfate (D_2SO_4). The current was 5 milliamperes. The anode and cathode were separated by a porous alumina crucible, as shown in figure 1. The separation was to prevent oxidizing agents that might be formed at the anode from reaching the cathode, which would permit the Pd to absorb higher concentrations of deuterium. Immediately after the absorption process, the wires were returned to the phenol formaldehyde holder for resistivity measurements at 4.2, 77, and 273 K to obtain $\rho(x)$ or the resistance $R(x)$.

For determination of the D/Pd atom ratios, each specimen was sectioned into five 1-centimeter pieces that corresponded to the positions on the phenol formaldehyde specimen holder. Then the deuterium was removed by heating each 1-centimeter section separately to 573 K in an evacuated system ($\sim 10^{-6}$ torr). Tests showed that less than 1 percent of the total gas concentration generally remained in the specimens. The specimens were weighed to three significant figures. The deuterium was expanded into and analyzed with a mass spectrometer, which is capable of 1 percent precision. The D/Pd atom ratios were then compared with their respective resistivity measurements.

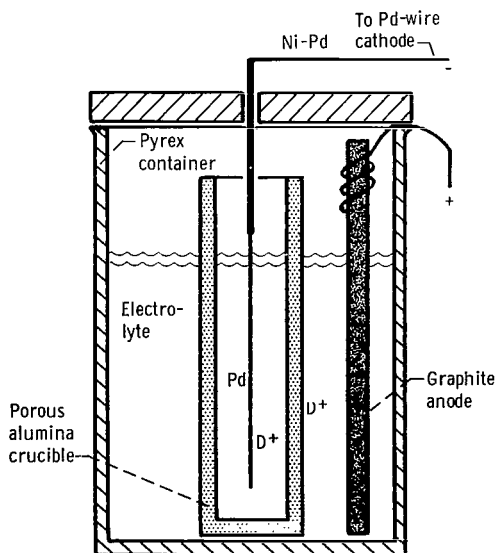
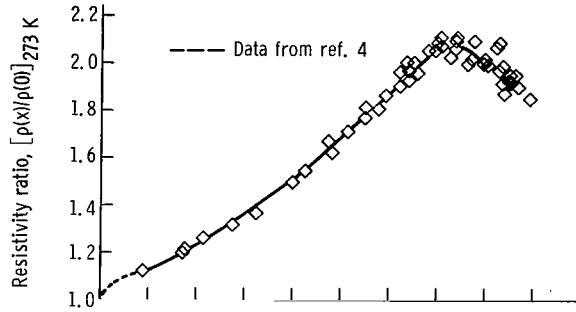


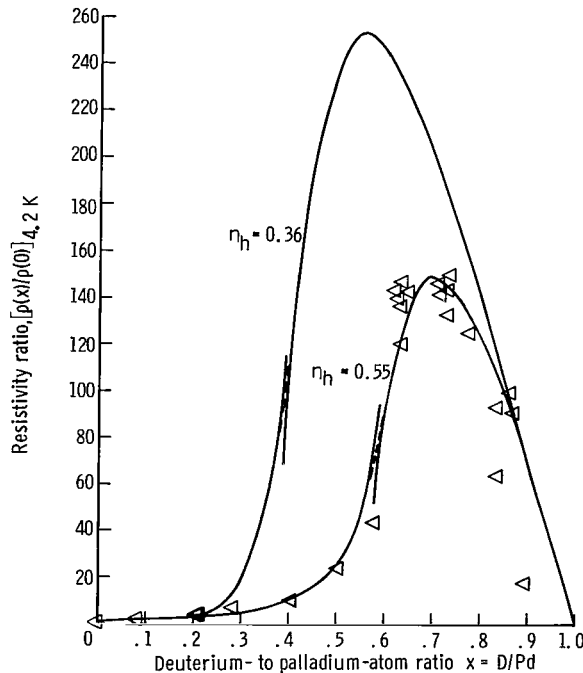
Figure 1. - Container used for deuterium absorption by palladium.

RESULTS

The results of resistivity measurements made at 4.2 and 273 K are shown in figure 2. As seen in figure 2(a), $[\rho(x)/\rho(0)]_{273K}$ and its derivative increase with x for $0.02 < x < 0.65$, and $[\rho(x)/\rho(0)]_{273K}$ reaches a maximum in the neighborhood of $x \approx 0.72$ and then decreases as $x \rightarrow 0.90$. At 4.2 K, the maximum in $[\rho(x)/\rho(0)]_{4.2K}$ appears to be near a value of 0.68 for the D/Pd atom ratio.



(a) Experimental curve of resistivity ratio at 273 K as function of deuterium-to-palladium-atom ratio.



(b) Resistivity ratio at 4.2 K. Curves calculated for number of d-band holes η_h equal to 0.36 and 0.55.

Figure 2. -Resistivity ratio as function of deuterium concentration in palladium.

Some of the scatter in the data may be attributed to two sources: (1) some hydrogen contamination, which varied between 3 and 8 percent of the total gas concentration, and (2) some evolution of the absorbed deuterium, for $x > 0.7$, between the resistivity measurements and mass spectrographic analysis. The time period for which evolution could take place was less than 20 minutes. (There is no evidence that evolution occurred at or below 77 K.) The possible gas loss for this time period is approximately a D/Pd atom ratio of 0.025, which is equivalent to a 2-percent change in $\rho(x)/\rho(0)$ at 273 K. The data shown in figure 2 include both the deuterium and the hydrogen impurity in x (i. e., (D + H)/Pd).

DISCUSSION

In figure 2(a), an experimental curve was drawn through the data points, whereas the curves in figure 2(b) were calculated for the values 0.36 and 0.55 for the number of holes n_h per Pd atom in the d-band. (The results for 77 K are not given because some octahedral-tetrahedral transitions occur during measurement.) The difference in the data at the two temperatures shown is attributed to the thermal contribution to the resistivity. At 4.2 K, both the thermal resistivity and that arising from lattice defects are expected to be small, so that their variation with deuterium concentration can be neglected. If x denotes the D/Pd atom ratio, the resistivity ratio $\rho(x)/\rho(0)$ at this temperature can therefore be written

$$\frac{\rho(x)}{\rho(0)} = 1 + \frac{\rho_D(x)}{\rho(0)} \quad (1)$$

where $\rho_D(x)$ is the contribution from disorder scattering by the deuterium randomly distributed among the octahedral sites in the host face-centered-cubic Pd lattice. This quantity is also the resistance ratio because the change in sample dimensions due to lattice expansion on absorption of D is negligible here. The average value of $\rho(0)$ for the samples used was determined to be 0.105 microhm-centimeter.

Magnetic susceptibility (ref. 5, p. 189) and electromigration (ref. 9) studies on the Pd-H system indicate that H exists in the Pd lattice as strongly screened positive ions, and presumably the same situation exists for D. The electronic structure of pure Pd was described by use of the Mott model (ref. 5, p. 189), in which the band structure is assumed to consist of a broad free-electron-like s-band overlapping with a narrow d-band, so that the Fermi level occurs near the top of the d-band. Thus, there are electrons in the s-band and an equal number of holes in the d-band. The assumption is made that initially the D atoms contribute their electrons to fill the holes in the d-band.

In a covalent bond picture, the electron is thought of as being shared with neighboring Pd atoms, which results in a strong screening of the D ion. The D ions, therefore, scatter a conduction electron only weakly, giving rise to a small initial slope (the change in slope on appearance of the β -phase, observed at higher temperatures, is greatly diminished at 4.2 K, which suggests that its origin is thermal rather than structural). As the holes in the d-band are filled, the electrons are instead contributed to the s-band, whose states are delocalized and, hence, do not screen as strongly. This lack of screening results in the sharp rise in resistance. Thus, the resistance is viewed as arising from scattering by three types of local structure, denoted by I, II, and III in the potential energy diagram of figure 3. Each of the three types is distributed randomly throughout the system. The screened coulomb potentials about the D ions have screening lengths a_d and a_s , with $a_d < a_s$.

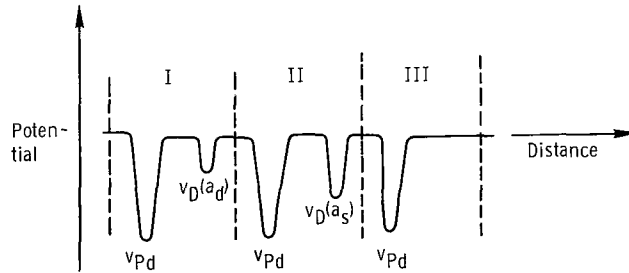


Figure 3. - Potentials associated with the three types of local structure assumed present in palladium-deuterium system. I, palladium atom associated with strongly screened deuterium ion, screening length a_d ; II, palladium atom associated with weakly screened ion, screening length a_s ; III, palladium atom associated with a vacancy.

If the current carried by the holes is neglected, the use of the Boltzmann equation and the assumption of an isotropic relaxation time τ lead to the usual expression

$$\rho = \frac{m_e^*}{N_e e^2 \tau} \quad (2)$$

where m_e^* is the effective mass and N_e the number of conduction electrons per unit volume. The inverse of the relaxation time can be written

$$\frac{1}{\tau} = \frac{1}{\tau_{s-s}} + \frac{1}{\tau_{s-d}} \quad (3)$$

However, the contribution from s-d scattering, proportional to the density of states at the Fermi level, goes to zero as the d-band fills. We therefore feel that s-d scattering cannot play a significant role in the sharp rise in $\rho(x)/\rho(0)$ with x and neglect it entirely.

When $1/\tau_{s-s}$ is evaluated in Born approximation (see appendix), the result for $\rho_D(x)$ is

$$\rho_D(x) = \frac{2}{3\pi} \frac{m_e^*{}^2 e^2}{\hbar^3} \frac{\Omega_o(x)}{[n_e(x)]^2} \left[f(4k_f^2 a_d^2) x_d (1 - x_d) \right. \\ \left. + f(4k_f^2 a_s^2) x_s (1 - x_s) + 2g(k_f, a_d, a_s) x_d x_s \right] \quad (4)$$

The quantity $\Omega_o(x)$ is the volume per Pd atom which is weakly dependent on x because of lattice expansion. Because the exact variation of lattice parameter with concentration is not important here, a simple linear expansion of the lattice parameter from 3.88×10^{-8} centimeter at $x = 0$, to 4.02×10^{-8} centimeter at $x = 0.60$, is assumed. The quantity $n_e(x)$ is the number of electrons per Pd atom in the s-band. The Fermi radius k_f is given by

$$k_f = \left[\frac{3\pi^2 n_e(x)}{\Omega_o(x)} \right]^{1/3}$$

while f and g are defined by

$$f(4k_f^2 a^2) = \ln(1 + 4k_f^2 a^2) - \frac{4k_f^2 a^2}{1 + 4k_f^2 a^2}$$

and

$$g(k_f, a_d, a_s) = \frac{a_s^2 \ln(1 + 4k_f^2 a_d^2) - a_d^2 \ln(1 + 4k_f^2 a_s^2)}{a_s^2 - a_d^2}$$

The coefficients x_d and x_s denote the number of D atoms per Pd atom contributing an electron to the d-band and s-band, respectively. Both depend implicitly on the total concentration x .

Expression (4) cannot be expected to be valid in the upper range of concentration (at and above the maximum in $[\rho(x)/\rho(0)]_{4, 2K}$) because the development of long-range order near $x = 1$, where the system takes on the sodium chloride structure, was not taken into account. The expression, therefore, overestimates the resistance in this range. If at $x = 1$, type I and II structures are regarded as constituting independent superlattices, then the resistance for $x \lesssim 1$ will arise from scattering by type II and III structures only. Proceeding as before in the evaluation of $1/\tau_{s-s}$ results in the high-charge expression (see appendix)

$$\rho_D(x) = \frac{2}{3\pi} \frac{m_e^*{}^2 e^2}{\hbar^3} \frac{\Omega_o(x) \cdot f(4k_f^2 a_s^2)}{[n_e(x)]^2} \frac{(x - n_h)(1 - x)}{1 - n_h} \quad (5)$$

where $x \gtrsim n_h$. The parameter n_h is the number of holes per Pd atom in the d-band at the initiation of charging; hence, it is also the number of octahedral sites per Pd atom available to the strongly screened D ions. The assumption of independent superlattices means that equation (5) underestimates the resistance in the range $x \gtrsim n_h$.

The terms x_d , x_s , and n_e are expected to have the qualitative behavior shown in figure 4. Note that $x_d + x_s = x$ and that $n_e(x) = n_e(0) + x_s$. The concentration x_f is that at which the d-band fills, and experiments by others (ref. 5, p. 316) on palladium - noble-metal alloys indicate x_f to be in the region of 0.55 to 0.60. On the basis of the

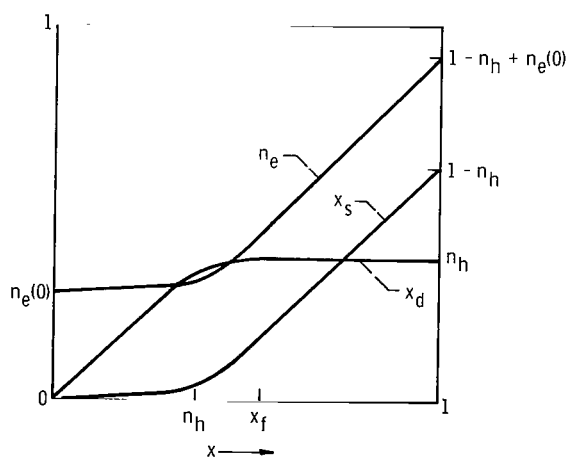


Figure 4. - Expected total-concentration dependence of quantities x_d , x_s , and n_e entering into equations (4) and (5).

de Haas - van Alphen measurements of Vuillemin (ref. 10) on pure Pd, $n_e(0) = 0.36$. If this value is also used for the number of holes, the upper curve in figure 2(b) is obtained. The dashed line indicates the continuous curve that would result from a more exact treatment of the onset of long-range order. The effective mass used, which was assumed independent of composition, was an average band mass of $0.49 m_e$ obtained from k_f and the Fermi level E_f for pure Pd. The quantity E_f was taken as 0.462 rydberg by using Segall's (ref. 11) band-structure calculations for copper and the similarity in the band structures of Pd and Cu (ref. 10). The quantity x_f was taken as 0.60, and a_d and a_s were determined by fitting equations (4) and (5) to the initial slope and final (extrapolated) slope, respectively. The fit over the entire concentration range is certainly not quantitative, but if the number of holes in the d-band is assumed to increase from 0.36 on charging, a much better fit is obtained, as shown in figure 2(b) by the curve for $n_h = 0.55$. Values for n_h in the range 0.55 to 0.60 are consistent with magnetic susceptibility data obtained by others on Pd-H (ref. 5, p. 316). The values for the screening lengths are $a_d = 0.26$ atomic units and $a_s = 1.11$ atomic units (at $x = 1$). This value for a_s is somewhat larger than the Thomas-Fermi value of 0.74 atomic units.

The authors are aware that the assumption of a spherical s-electron Fermi surface neglects the appreciable anisotropy, which extends to about 30 percent (ref. 10). However, the Mott model, with the interpretation of the de Haas - van Alphen work that $n_e(0) = n_h(0) = 0.36$, appears to work well in explaining the transport properties of the Pd - noble-metal alloys (ref. 12). The apparent failure of the rigid-band model for Pd-D indicated herein suggests that further work on this system would be of interest. In particular, a band-structure calculation could be done for the ordered structure $x = 1$ to obtain $n_e(1)$. The rigid-band model predicts one s-electron per Pd atom at $D/Pd = 1$ or at $H/Pd = 1$, whereas the present analysis would indicate 0.81 electron per atom. In conjunction, a de Haas - van Alphen experiment could be conducted, which would be dependent, however, on overcoming present experimental difficulty in consistently obtaining high D/Pd ratios.

CONCLUSIONS

The direct-current electrical resistivity of the palladium-deuterium (Pd-D) system was measured to a deuterium- to palladium-atom ratio of 0.9. Analysis of the resistivity as a function of atom ratio at 4.2 K indicated that on addition of deuterium, the number of holes in the d-band (per Pd atom) takes on the value of 0.55 to 0.60, compared with the value of 0.36 for pure Pd, which is based on recent experimental and theoretical work by

others. This result suggests that the rigid-band model is not valid for the Pd-D interstitial solid solution, in contrast to the Pd - noble-metal alloy systems.

Lewis Research Center,

National Aeronautics and Space Administration,

Cleveland, Ohio, October 16, 1968,

129-03-15-01-22.

APPENDIX - EVALUATION OF INVERSE OF RELAXATION TIME

The inverse of the relaxation time τ_{s-s} for scattering of an s-electron at the Fermi surface back into an s-state by a single scatterer is (ref. 5, p. 247)

$$\frac{1}{\tau_{s-s}} = \frac{\Omega}{4\pi^2\hbar} \int_{\text{s-surface}} dS (1 - \cos \theta) |v_{\underline{k}'\underline{k}}|^2 \frac{1}{|\nabla E_f|} \quad (A1)$$

$$= \frac{\Omega}{2\pi\hbar} k_f^2 \left(\frac{dE}{dk} \right)_{k=k_f}^{-1} \int_0^\pi d\theta (1 - \cos \theta) \sin \theta |v_{\underline{k}'\underline{k}}|^2$$

The integral is taken over all scattering angles θ between the initial state \underline{k} and final state \underline{k}' . The matrix element $v_{\underline{k}'\underline{k}}$ is

$$\int_{\Omega} d\underline{r} \varphi_{\underline{k}'}^*(\underline{r}) v(\underline{r}) \psi_{\underline{k}}(\underline{r})$$

where $\psi_{\underline{k}}$ is the initial state in the presence of the scattering potential $v(\underline{r})$, and $\varphi_{\underline{k}'}$ is the final state in the absence of v . The s-band wave functions are assumed to be plane waves. In the Born approximation, $\psi_{\underline{k}}$ is taken equal to $\varphi_{\underline{k}}$ in evaluating $v_{\underline{k}'\underline{k}}$. Hence,

$$v_{\underline{k}'\underline{k}} = \frac{1}{\Omega} \int_{\Omega} d\underline{r} e^{-i(\underline{k}'-\underline{k}) \cdot \underline{r}} v(\underline{r}) \quad (A2)$$

Since a perfectly periodic potential has no resistance, the contribution from each type of local structure of figure 3 is considered to arise from the difference between the actual potential and the average potential there. The average potential is

$$v_{av} = [v_{Pd} + v_D(a_d)]x_d + [v_{Pd} + v_D(a_s)]x_s + v_{Pd}(1 - x_d - x_s)$$

Hence, the scattering potentials are

Type I:

$$\begin{aligned}
v(\underline{r}) &= v - v_{av} \\
&= \left[v_{Pd} + v_D(a_d) \right] - \left[v_{Pd} + x_d v_D(a_d) + x_s v_D(a_s) \right] \\
&= (1 - x_d) v_D(a_d) - x_s v_D(a_s)
\end{aligned}$$

Type II:

$$v(\underline{r}) = (1 - x_s) v_D(a_s) - x_d v_D(a_d)$$

Type III:

$$v(\underline{r}) = -x_d v_D(a_d) - x_s v_D(a_s)$$

The total contribution to $1/\tau_{s-s}$ from each type of scatterer consists of a term of the form of equation (A1) with the appropriate scattering potential, weighted by the number of each type. Denoting matrix elements by $\langle \rangle$ and integration over the scattering angle by $\overline{(\quad)}$ gives

$$\begin{aligned}
\frac{1}{\tau_{s-s}} &= \frac{\Omega N_{Pd}}{2\pi\hbar} k_f^2 \left(\frac{dE}{dk} \right)_{k=k_f}^{-1} \left\{ \overline{|\langle v_D(a_d) \rangle|^2} x_d (1 - x_d) + \overline{|\langle v_D(a_s) \rangle|^2} x_s (1 - x_s) \right. \\
&\quad \left. + 2 \operatorname{Re} \left[\overline{\langle v_D(a_d) \rangle \langle v_D(a_s) \rangle^*} \right] x_d x_s \right\} \quad (A3)
\end{aligned}$$

where N_{Pd} is the number of Pd atoms in the system. The appropriate integrals can be evaluated in a straightforward manner, the result being equation (4) of the text.

In the high-charge region, the resistance is assumed to arise mostly from the presence of vacancies in a superlattice of type II structures. The scattering arises from fluctuations in an average potential:

$$v_{av} = v_{Pd} + \frac{x_s}{1 - n_h} v_D(a_s)$$

The scattering potentials are now

Type II:

$$v(\underline{r}) = \left(1 - \frac{x_s}{1 - n_h}\right) v_D(a_s)$$

Type III:

$$v(\underline{r}) = -\frac{x_s}{1 - n_h} v_D(a_s)$$

There are x_s type II scatterers and $1 - x$ type III scatterers per Pd atom. Therefore,

$$\frac{1}{\tau_{s-s}} = \frac{\Omega N_{Pd}}{2\pi\hbar} k_f^2 \left(\frac{dE}{dk}\right)_{k=k_f}^{-1} \left[\overline{|\langle v_D(a_s) \rangle|^2} \left(1 - \frac{x_s}{1 - n_h}\right)^2 x_s + \overline{|\langle v_D(a_s) \rangle|^2} \left(\frac{x_s}{1 - n_h}\right)^2 (1 - x) \right] \quad (A4)$$

Now, $x_d + x_s = x$, and from figure 4, $x_d \approx n_h$ for $x \gg n_h$. Thus, using $x_s = x - n_h$ results in

$$\frac{1}{\tau_{s-s}} = \frac{\Omega N_{Pd}}{2\pi\hbar} k_f^2 \left(\frac{dE}{dk}\right)_{k=k_f}^{-1} \overline{|\langle v_D(a_s) \rangle|^2} \frac{(x - n_h)(1 - x)}{1 - n_h} \quad x \gg n_h \quad (A5)$$

Substituting the explicit expression for $\overline{|\langle v_D(a_s) \rangle|^2}$ leads to equation (5) of the text.

REFERENCES

1. Worsham, J. E., Jr.; Wilkinson, M. K.; and Schull, C. G.: Neutron-Diffraction Observations on the Palladium-Hydrogen and Palladium-Deuterium Systems. *J. Phys. Chem. Solids*, vol. 3, 1957, pp. 303-310.
2. Maeland, Arnulf J.; A Neutron-Diffraction Study of the α Phase in the Palladium-Gold-Hydrogen and Palladium-Gold-Deuterium Systems. *Can. J. Phys.*, vol. 46, Jan. 15, 1968, pp. 121-124.
3. Barton, J. C.; Lewis, F. A.; and Woodward, I.: Hysteresis of the Relationships Between Electrical Resistance and the Hydrogen Content of Palladium. *Trans. Faraday Soc.*, vol. 59, 1963, pp. 1201-1207.
4. Flanagan, Ted B.: Absorption of Deuterium by Palladium. *J. Phys. Chem.*, vol. 65, no. 2, Feb. 1961, pp. 280-284.
5. Mott, N. F.; and Jones, H.: *The Theory of the Properties of Metals and Alloys*. Dover Publications, Inc., 1958.
6. Schindler, A. I.; Smith, R. J.; and Kammer, E. W.: Low Temperature Dependence of the Electrical Resistivity and Thermoelectric Power of Palladium and Palladium-Nickel Alloys Containing Absorbed Hydrogen. *Proceedings of the Tenth International Congress on Refrigeration. Vol. I.* Pergamon Press, 1960, pp. 74-79.
7. Ferguson, G. A., Jr.; Schindler, A. I.; Tanaka, T.; and Morita, T.: Neutron Diffraction Study of Temperature-Dependent Properties of Palladium Containing Absorbed Hydrogen. *Phys. Rev.*, vol. 137A, no. 2, Jan. 18, 1965, pp. 483-487.
8. Smith, Robert J.: Anomalous Electrical Resistivity of Palladium-Deuterium System Between 4.2^o and 300^o K. NASA TN D-2568, 1965.
9. Barrer, Richard M.: *Diffusion in and Through Solids*. Cambridge University Press, 1941, p. 220.
10. Vuillemin, Joseph J.: De Haas-van Alphen Effect and Fermi Surface in Palladium. *Phys. Rev.*, vol. 144, no. 2, Apr. 15, 1966, pp. 396-405.
11. Segall, Benjamin: Fermi Surface and Energy Bands of Copper. *Phys. Rev.*, vol. 125, no. 1, Jan. 1, 1962, pp. 109-122.
12. Dugdale, J. S.; and Guénault, A. M.: The Low Temperature Transport Properties of the Palladium-Silver Alloy Series. *Phil. Mag.*, vol. 13, no. 123, Mar. 1966, pp. 503-513.

FIRST CLASS MAIL

POSTMASTER: If Undeliverable (Section 158
Postal Manual) Do Not Return

"The aeronautical and space activities of the United States shall be conducted so as to contribute . . . to the expansion of human knowledge of phenomena in the atmosphere and space. The Administration shall provide for the widest practicable and appropriate dissemination of information concerning its activities and the results thereof."

— NATIONAL AERONAUTICS AND SPACE ACT OF 1958

NASA SCIENTIFIC AND TECHNICAL PUBLICATIONS

TECHNICAL REPORTS: Scientific and technical information considered important, complete, and a lasting contribution to existing knowledge.

TECHNICAL NOTES: Information less broad in scope but nevertheless of importance as a contribution to existing knowledge.

TECHNICAL MEMORANDUMS: Information receiving limited distribution because of preliminary data, security classification, or other reasons.

CONTRACTOR REPORTS: Scientific and technical information generated under a NASA contract or grant and considered an important contribution to existing knowledge.

TECHNICAL TRANSLATIONS: Information published in a foreign language considered to merit NASA distribution in English.

SPECIAL PUBLICATIONS: Information derived from or of value to NASA activities. Publications include conference proceedings, monographs, data compilations, handbooks, sourcebooks, and special bibliographies.

TECHNOLOGY UTILIZATION PUBLICATIONS: Information on technology used by NASA that may be of particular interest in commercial and other non-aerospace applications. Publications include Tech Briefs, Technology Utilization Reports and Notes, and Technology Surveys.

Details on the availability of these publications may be obtained from:

**SCIENTIFIC AND TECHNICAL INFORMATION DIVISION
NATIONAL AERONAUTICS AND SPACE ADMINISTRATION
Washington, D.C. 20546**